Effect of M_xO_y (M= Si, Ti, Ca, Mg) Dopants on Solid-State Sintering of Yttrium Aluminium Garnet

A Thesis Submitted in Partial Fulfillment of the Requirements for the Degree of

Bachelor of Technology

by

Udipta Thakur (Roll No. 108CR041)

Department of Ceramic Engineering
National Institute of Technology Rourkela
Rourkela, Odisha-769008

Effect of M_xO_y (M= Si, Ti, Ca, Mg) Dopants on Solid-State Sintering of Yttrium Aluminium Garnet

A Thesis Submitted in Partial Fulfillment of the Requirements for the Degree of

Bachelor of Technology

by

Udipta Thakur (Roll No. 108CR041)

Supervisor:

Prof. Debasish Sarkar

Department of Ceramic Engineering
National Institute of Technology Rourkela
Rourkela, Odisha-769008

Table of Contents

List of Figures

ACKNOWLEDGEMENT

I express my deep sense of gratitude and indebtedness to my project supervisor, Dr. Debasish Sarkar, Associate Professor, National Institute of Technology for his constant guidance, valuable suggestions and constructive criticisms throughout the span of my project work. It wouldn't have been possible for me to bring out this project report without his support and constant encouragement.

I take this opportunity to thank Prof. J. Bera, Head of the Department, Ceramic Engineering for his guidance and support. I'm highly obliged to my departmental faculty members Prof. H.S. Maity, Prof. S. Bhattacharya, Prof. R. Sarkar, Prof. S.K. Pratihar, Prof. S.K. Pal, Prof. R. Mazumdar, Prof. B.B. Nayak, Prof. S. Behera, Prof. Sunipa Bhattacharya, Prof. Dasgupta for their valuable suggestions and guidance at different phases of my project work.

I would also like to thank the Research Scholars and the Laboratory Staff members of the Ceramic Engineering Department for their constant help and support in carrying out various lab experiments and analysis work.

Udipta Thakur

108CR041

National Institute of Technology Rourkela

CERTIFICATE

This is to certify that the thesis entitled *"**Effect of M_xO_y (M= Si, Ti, Ca, Mg) Dopants on Solid-State Sintering of Yttrium Aluminium Garnet**"* submitted by Mr**. Udipta Thakur** in partial fulfillment of the requirements for the award of **Bachelor of Technology** degree in **Ceramic Engineering** at National Institute of Technology, Rourkela is an authentic work carried out by him under my supervision and guidance.

To the best of my knowledge, the matter embodied in this thesis has not been submitted to any other University/Institute for the award of any degree or diploma.

Date:

Prof. Debasish Sarkar
Department of Ceramic Engineering
National Institute of Technology
Rourkela-769008

Abstract

Polycrystalline Yttrium Aluminium Garnet (YAG) ceramic has been prepared by solid-state reactive sintering route. Nano-sized Al_2O_3 (120nm) and Y_2O_3 (100nm) powders along with 0.1 wt.% of the oxide dopants (SiO_2,TiO_2,CaO,MgO) were mixed through ball milling, pelletized and sintered at different sintering temperatures such as 1350^{o}C, 1450^{o}C, 1550^{o}C and 1650^{o}C with varying amount of soaking time for each peak temperature. X-ray diffraction analysis has been carried to identify the phase transformation and change in crystallite size of the samples with varying temperature, time and dopant used. Scanning Electron Microscopy was done to study the morphology and grain size dependence of the synthesized YAG ceramic on the sintering parameters and type of dopant used. Dilatometry was carried out with powder precursors to track the transformation of low temperature phases such as YAM, YAP to YAG phase. Other characterizations such as Bulk Density, Apparent Porosity and Shrinkage measurements were done to study the amount of densification and pore concentration achieved specific to the dopant used at different sintering temperatures.

Chapter 1

Introduction

1.1 Structure of Yttrium Aluminium Garnet

Garnet has a complex cubic structure with a formula $X_3Y_2Z_3O_{12}$.

- X site has a distorted 8-fold coordination.
- Y site has 6-fold octahedral coordination.
- Z site has tetrahedral coordination.

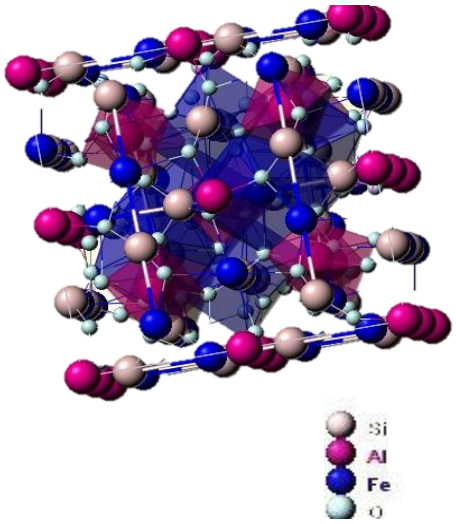

Fig. 1.1 *The garnet crystal structure* [1]

This tetrahedral site is typically occupied by silica tetrahedrons in the case of most natural garnets, such as Almandine: $Fe_3Al_2(SiO_4)_3$

Yttrium **A**luminum **G**arnet has a coupled substitution. Starting with almandine $Fe_3Al_2(SiO_4)_3$, the Fe is replaced with Y, and the charge balance is maintained by replacing the Si with tetrahedrally coordinated Al. This gives a formula of $\mathbf{Y_3Al_2(AlO_4)_3}$, or $\mathbf{Y_3Al_5O_{12}}$.[1]

1.2 Phase Diagram for the Y_2O_3-Al_2O_3 system:

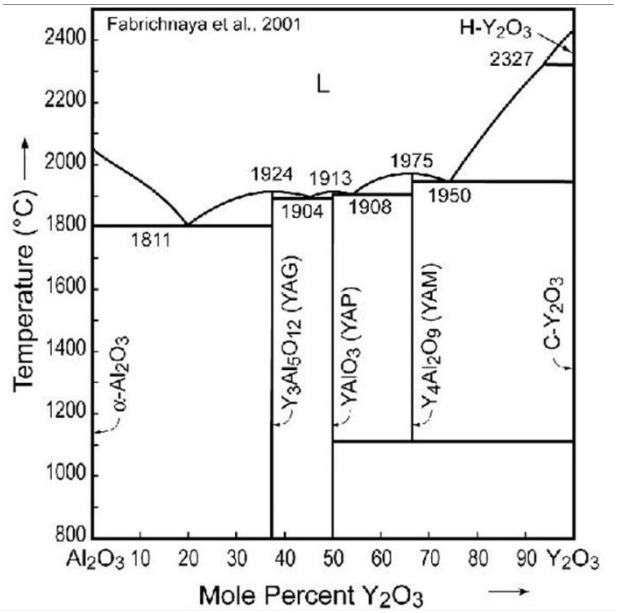

Transformation Reactions: [2]

$$2Y_2O_3 + Al_2O_3 \longrightarrow Y_4Al_2O_9 \text{ (YAM)}$$

$$Y_4Al_2O_9 \text{ (YAM)} + Al_2O_3 \longrightarrow YAlO_3 \text{ (YAP)}$$

$$YAlO_3 + Al_2O_3 \longrightarrow Y_3Al_5O_{12} \text{ (YAG)}$$

***Fig. 1.2** Phase Diagram for the Y_2O_3-Al_2O_3 system* [3]

Figure 1.2 is the phase diagram for the Y_2O_3-Al_2O_3 system. $Y_3Al_5O_{12}$ (YAG) is a line compound which has important consequences while processing; any kind of presence of non-stoichiometry in the material is detected as a secondary phase scattering site which may restrict the optical transmission of the material. [3]

1.3 Solid-State Sintering

The solid-state sintering phenomena in polycrystalline materials are considerably complex because of the availability of several matter transport paths and the presence of grain boundaries.

Matter transport in solid-state sintering can occur by at least six different paths which define the mechanisms of sintering. In practice, more than one mechanism may operate during any given regime of sintering, and the occurrence of multiple mechanisms makes analysis of sintering rates and the determination of sintering mechanisms difficult. Perhaps the most important consequence of the grain boundaries is the occurrence of grain growth and pore growth during sintering, a process normally referred to as coarsening. The coarsening process provides an alternative route by which the free energy of the powder system can be reduced, therefore, it reduces the driving force for densification. [4]

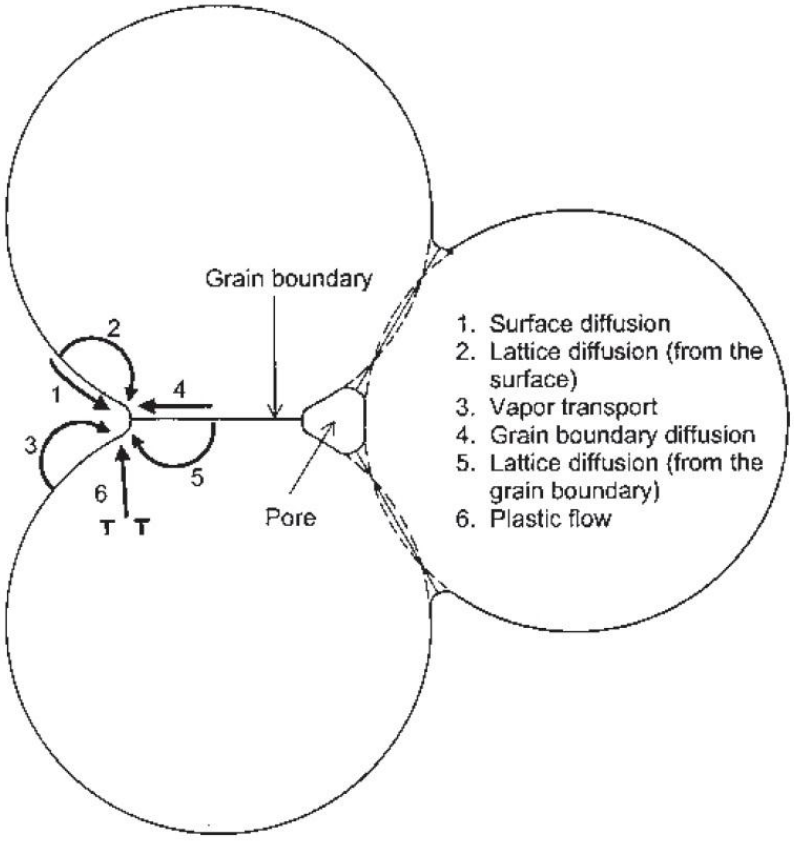

Fig.1.3 *Six different mechanisms of matter transport in solid-state sintering.* [4]

Chapter 2

Literature Review

2.1 YAG as a gain material in LASERS

YAG has acquired immense popularity being the most commonly used laser gain host and has been popular for the use as a substrate material in optical components. YAG is a stable compound, mechanically tough, physically hard, optically isotropic, and transparent for optical ranges from below 300nm to beyond 4 microns.

2.2 Advantages of polycrystalline YAG ceramic over single crystal YAG

- ✓ As compared to single crystal YAG, its polycrystalline counterpart can be highly doped.
- ✓ YAG ceramic requires less process time and average skills to produce as contrary to single crystal YAG.
- ✓ Polycrystalline YAG ceramic is a more amenable product for mass production hence making it cheaper out of the two varieties.
- ✓ Ceramic YAG has a comparable light scattering loss.
- ✓ Larger size rods can be fabricated in the case of YAG ceramic.
- ✓ Unique composite structure designs can be achieved.

- ✓ It has superior doping profiles as compared to single crystal YAG.

2.3 Advantages of Solid-State Reaction (SSR) sintering over other routes

- ✓ Commercially available powders can be used.
- ✓ It is easier to implement for materials requiring dopants.

2.4 Paper Reviews

- ✓ *Yang et al.* followed the SSR route to fabricate Nd:YAG ceramics under vacuum using α-Al_2O_3,Y_2O_3 and Nd_2O_3 as starting materials and both MgO and TEOS as sintering additives. A comparison was drawn by preparing Nd:YAG with either MgO or TEOS as sintering aid. Morphology and microstructure of the ceramic was studied. Optical transmittance properties of Nd:YAG with varying sintering temperature and amount of additives used.[5]
- ✓ *Quing et al.*'s work demonstrates the solid state reactive sintering approach in the preparation of YAG ceramics. In this work Al_2O_3 and Y_2O_3 were mixed in stoichiometric amounts and phase formation takes place during sintering. [6]
- ✓ *Kochawattana et al.* studied the activation energy for grain growth and densification of pure YAG, Nd:YAG and the effect of SiO_2 doping on the densification of these ceramics.[7]
- ✓ *Esposito et al.* reports the microstructural and optical properties of YAG ceramics synthesized through SSR route by using micrometer sized Y_2O_3, Al_2O_3 and Nd_2O_3. Two processing routes i.e. cold isostatic pressing and slip casting were employed and

comparison between microstructural properties between green and vacuum sintered bodies were done.[8]

- ✓ *Li et al.*'s work demonstrates the solid state reactive sintering approach in the preparation of YAG ceramics. In this work Al_2O_3 and Y_2O_3 were mixed in stoichiometric amounts and phase formation takes place during sintering. [9]
- ✓ According to reports by *Wen et al.*, highly pure nanometric yttria powder was synthesized though wet chemical route. Taking this nanometric yttria and commercial grade alumina powder, YAG was prepared through solid-state reactive sintering method. Characterizations were done to investigate the results obtained. [10]
- ✓ *Yang et al.* fabricated high quality, transparent Nd:YAG through reactive sintering method under vacuum. SiO_2 and MgO were used as co-dopants (sintering additives). The microstructure, morphology and optical properties of the fabricated Nd:YAG were studied. It was inferred that the use of SiO_2 and MgO as co-dopants can greatly improve the densification rate of the material. [11]
- ✓ *Liu et al.* prepared Nd:YAG powder through co-precipitation method using MgO as a sintering additive/dopant. Effect of various amounts of MgO additive on the synthesis route was studied. Nd:YAG ceramics were prepared by vacuum sintering the Nd:YAG powders and optical property testing was done. [12]

Chapter 3

Experimental Procedure

3.1 Flowchart of the synthesis route

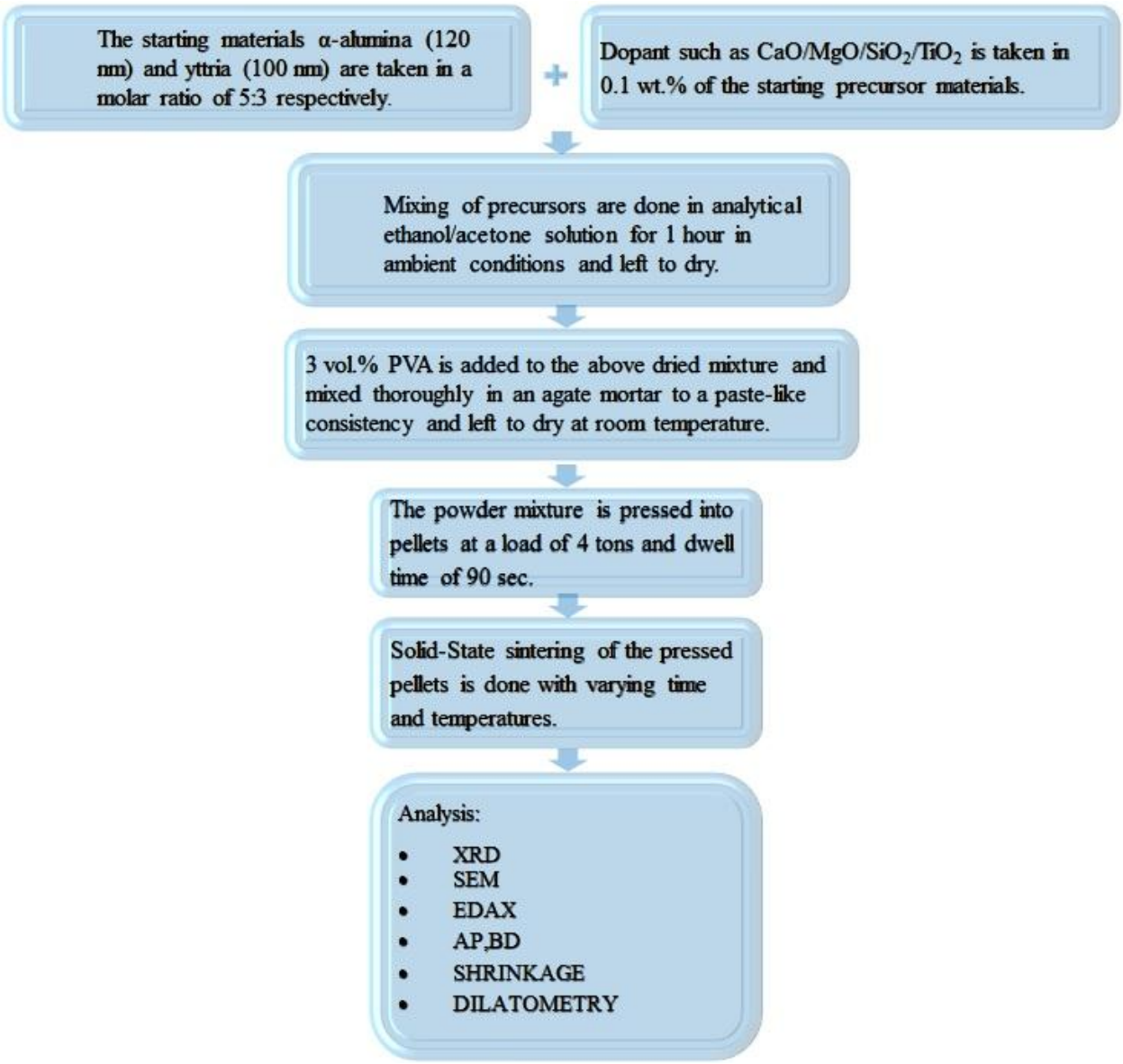

Fig. 3.1 *Flowchart for YAG synthesis.*

3.2 Specifications of the precursor materials

Table 3.1 *Specifications and brand of reagents used for YAG preparation*

Reagent	Specifications
α-Al_2O_3	120 nm
Y_2O_3	100 nm
SiO_2	380 nm
TiO_2	Alkem Laboratories
$Ca(NO_3)_2.4H_2O$	Loba Chemie (99% Assay)
$Mg(NO_3)_2.6H_2O$	Loba Chemie (99% Assay)

3.3 Batch Calculations

Molecular weight of α-Alumina (Al_2O_3) = 101.96 g mol^{-1}

Molecular weight of Yttria (Y_2O_3) = 225.81 g mol^{-1}

Molecular weight of Yttrium Aluminium Garnet ($Y_3Al_5O_{12}$) = 596.70 g mol^{-1}

Reaction:

$$3Y_2O_3 + 5Al_2O_3 \longrightarrow 2Y_3Al_5O_{12}$$

If 'M' grams of batch is to be prepared

No. of moles of YAG to be prepared = M/596.70 g mol^{-1} = X moles (suppose)

Hence,

No. of moles of α-Alumina (Al_2O_3) to be taken = (5/2) * X moles

No. of moles of Yttria (Y_2O_3) to be taken = (3/2) * X moles

Amount (weight) of α-Alumina (Al_2O_3) to be taken = [(5/2) * X moles * 101.96 g mol^{-1}] grams

Amount (weight) of Yttria (Y_2O_3) to be taken = [(3/2) * X moles * 225.81 g mol^{-1}] grams

Amount of M_xO_y (M=Si, Ti, Ca, Mg) dopant used = 0.1 wt. % of YAG batch= 0.1 wt. % of 'M'

Therefore, weights of the respective reagents are calculated accordingly.

3.3 Working Procedure

Step 1:

Batch calculations were done and the required amount of starting materials (Al_2O_3, Y_2O_3, M_xO_y) were weighed over an electronic weighing machine and care was taken over the use of clean apparatus whether it is the weighing spatula, weighing machine or paper over which the sample is weighed.

Step 2:

Milling was done in a planetary ball mill "Fritsch Pulverisette 6" with ZrO_2 balls as the grinding media. The ball mill operates with two covered bowls made of ZrO_2 partially filled with ethanol as the milling medium. Two sets of balls were taken of different sizes in each bowl for effective milling. Each bowl comprised of 15 big balls (20mm) and 15 small balls (10 mm) immersed in ethanol. The weighed materials were divided into two parts for each of the ZrO_2 bowls. With the bowls in position and the hood closed, the planetary ball mill was programmed to run at 300 RPM for 12 hours.

Step 3:

The milled precursors were taken out of the ZrO_2 bowl over a petri dish and were allowed to dry off in ambient conditions.

Step 4:

The dried milled powder was taken on an agate mortar and grinded with the help of a pestle. A binder was required for the further processing of the material that could easily burnout at a relatively lower temperature while sintering without hampering the composition or

microstructure of the material. Hence, an organic binder such a Polyvinyl Alcohol (3 vol. %) was taken. An arbitrary amount of the binder was added to the milled powder in the agate mortar and mixed to attain a paste like consistency. Further mixing is done to ensure uniform mixing of the material and PVA and was kept under an IR lamp to let the material dry off. After drying the material is ground into fine powder in the agate mortar itself and then stored in plastic zip pouch for further processing.

Step 5:

The powder is then weighed over the electronic weighing machine and separated into batches of 0.6 gram each which will be pressed into pellets.

Step 6:

The 0.6 gram batches of powder were pressed into pellets in a die-punch system having a diameter of 12.1 mm. Pressing was done with the help of CARVER press with the pressing specifications: Load: 4 tons; Dwell Time: 90 seconds. Stearic acid and acetone were used for lubrication and cleaning purposes respectively.

Step 7:

The pressed pellets were sintered at temperatures 1350 ^{o}C, 1450 ^{o}C, 1550 ^{o}C and 1650 ^{o}C with a variable soaking time of 2,4,6 and 8 hours at each of the temperatures. The furnace employed for sintering of the pellets was Raising Hearth Furnace with a rated capacity of 1700^{o}C. The entire heating schedule was a 4 step process. Heating was done from the ambient temperature to 650 ^{o}C at a rate of 3^{o}C/min. At 650 ^{o}C soaking was done for 1 hour to ensure complete binder removal. Heating is continued at a rate of 3 ^{o}C/min to the final sintering temperature where soaking is done for the requisite amount of time. After the 4 step process is over the program ends and the furnace is allowed to cool for 1 day.

Step 8:

The pellets were taken out of the furnace and were subjected to various characterization procedures such as X-Ray Diffraction, Dilatometry, Scanning Electron Microscopy, Bulk Density, Apparent Porosity and Shrinkage measurements.

Chapter 4

Results & Discussions

4.1 X-Ray Diffraction Analysis

4.1.1 Analysis on YAG without dopants

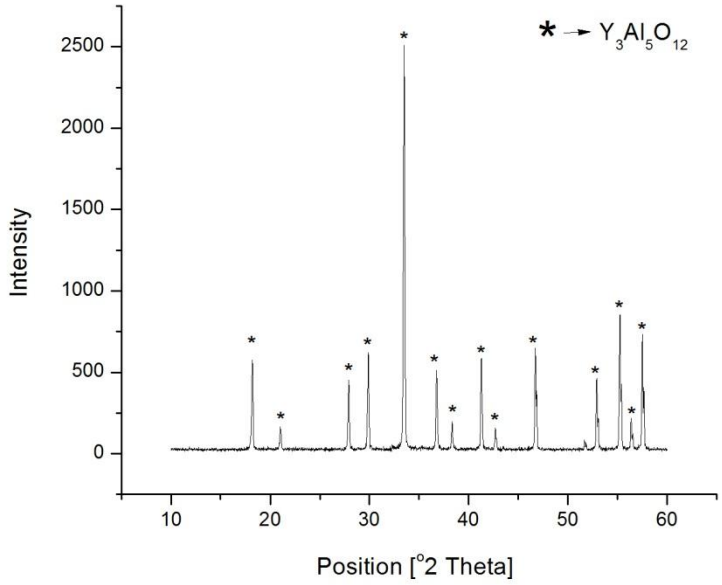

Fig 4.1(a) *XRD graph of sample sintered at 1650^{o}C for 8 hours.*

Table 4.1(a) *Pattern list of identified compounds for sample sintered at 1650^{o}C for 8 hours.*

Ref. Code	Score	Compound Name	Displacement [°2Th.]	Scale Factor	Chemical Formula
79-1891	92	Yttrium Aluminum Oxide	0.138	0.898	$Y_3Al_5O_{12}$

Figure 4.1(a) shows that pure YAG phase has been obtained by sintering the sample at 1650^{o}C for 8 hours without any sign of YAM and YAP phase formation. This ensures that complete transformation has taken place.

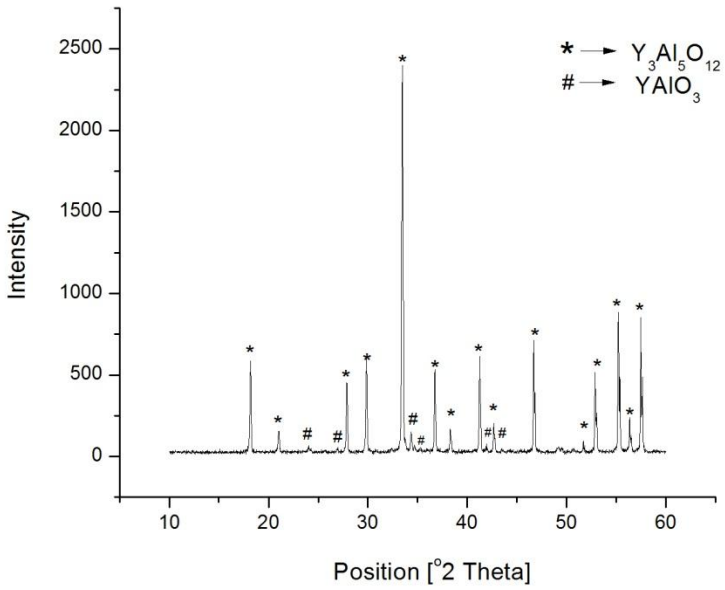

Fig 4.1(b) *XRD graph of sample sintered at 1550^{o}C for 8 hours.*

Table 4.1(b) *Pattern list of identified compounds for sample sintered at 1550^{o}C for 8 hours.*

Ref. Code	Score	Compound Name	Displacement [°2Th.]	Scale Factor	Chemical Formula
79-1891	87	Yttrium Aluminum Oxide	0.110	1.003	$Y_3Al_5O_{12}$
11-0662	39	Aluminum Yttrium Oxide	0.002	0.035	$AlYO_3$

Figure 4.1(b) shows that there are two phases in the system, namely YAG (major phase) and YAP (minor phase) for the sample sintered at 1550^{o}C for 8 hours. It indicates partial transformation of YAP phase to YAG phase at this temperature.

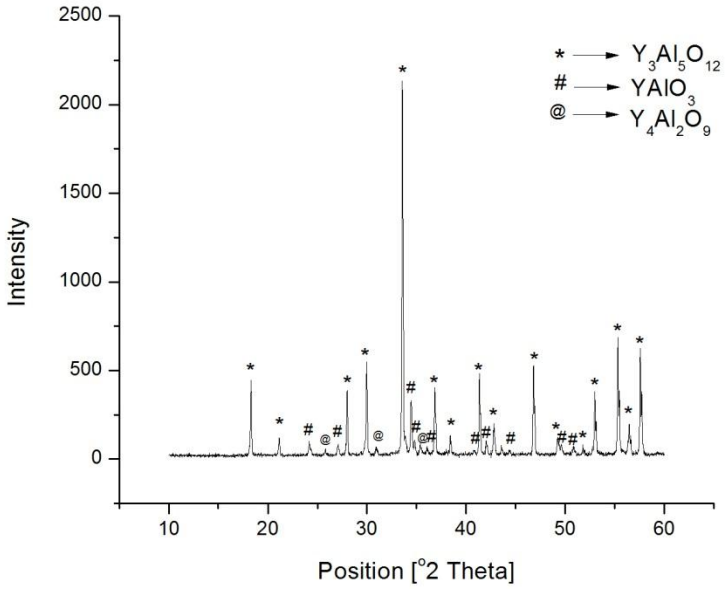

Fig 4.1(c) *XRD graph of sample sintered at 1450^{o}C for 8 hours*

Table 4.1(c) *Pattern list of identified compounds for sample sintered at 1450^{o}C for 8 hours.*

Ref. Code	Score	Compound Name	Displacement [°2Th.]	Scale Factor	Chemical Formula
73-1370	69	Aluminum Yttrium Oxide	0.152	0.769	$Al_5Y_3O_{12}$
70-1677	35	Yttrium Aluminum Oxide	0.130	0.081	$YAlO_3$
34-0368	7	Aluminum Yttrium Oxide	0.066	0.027	$Al_2Y_4O_9$

Figure 4.1(c) indicates the presence of all three important phases of the Y_2O_3-Al_2O_3 system i.e. YAM, YAP and YAG.YAG is the major phase in the system followed by YAP and then YAM.

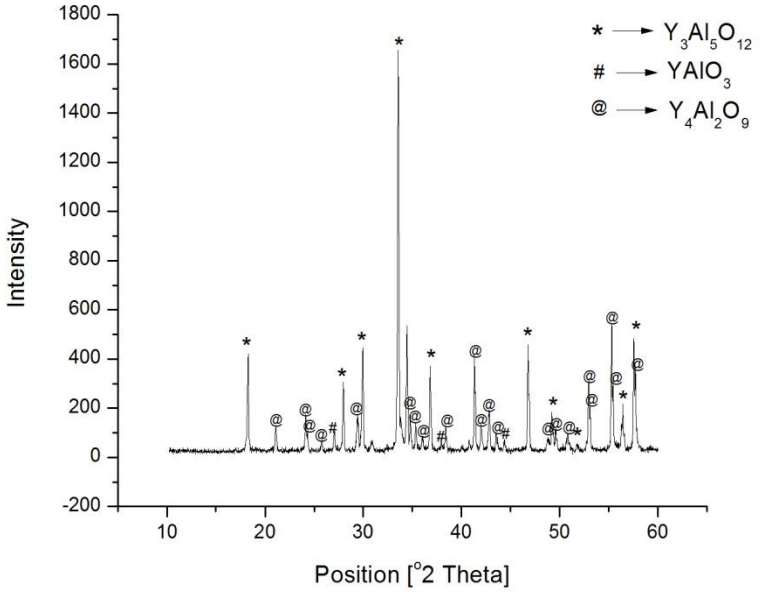

Fig 4.1(d) *XRD graph of sample sintered at 1350°C for 8 hours*

Table 4.1(d) *Pattern list of identified compounds for sample sintered at 1350°C for 8 hours.*

Ref. Code	Score	Compound Name	Displacement [°2Th.]	Scale Factor	Chemical Formula
72-1853	63	Yttrium Aluminum Oxide	0.152	0.764	$Y_3Al_5O_{12}$
70-1677	46	Yttrium Aluminum Oxide	0.129	0.185	$YAlO_3$
83-0934	13	Aluminum Yttrium Oxide	0.072	0.075	$Al_2Y_4O_9$

Figure 4.1(d) shows the abundance of partially transformed YAM phase at 1350°C with YAP and YAG in the composition.

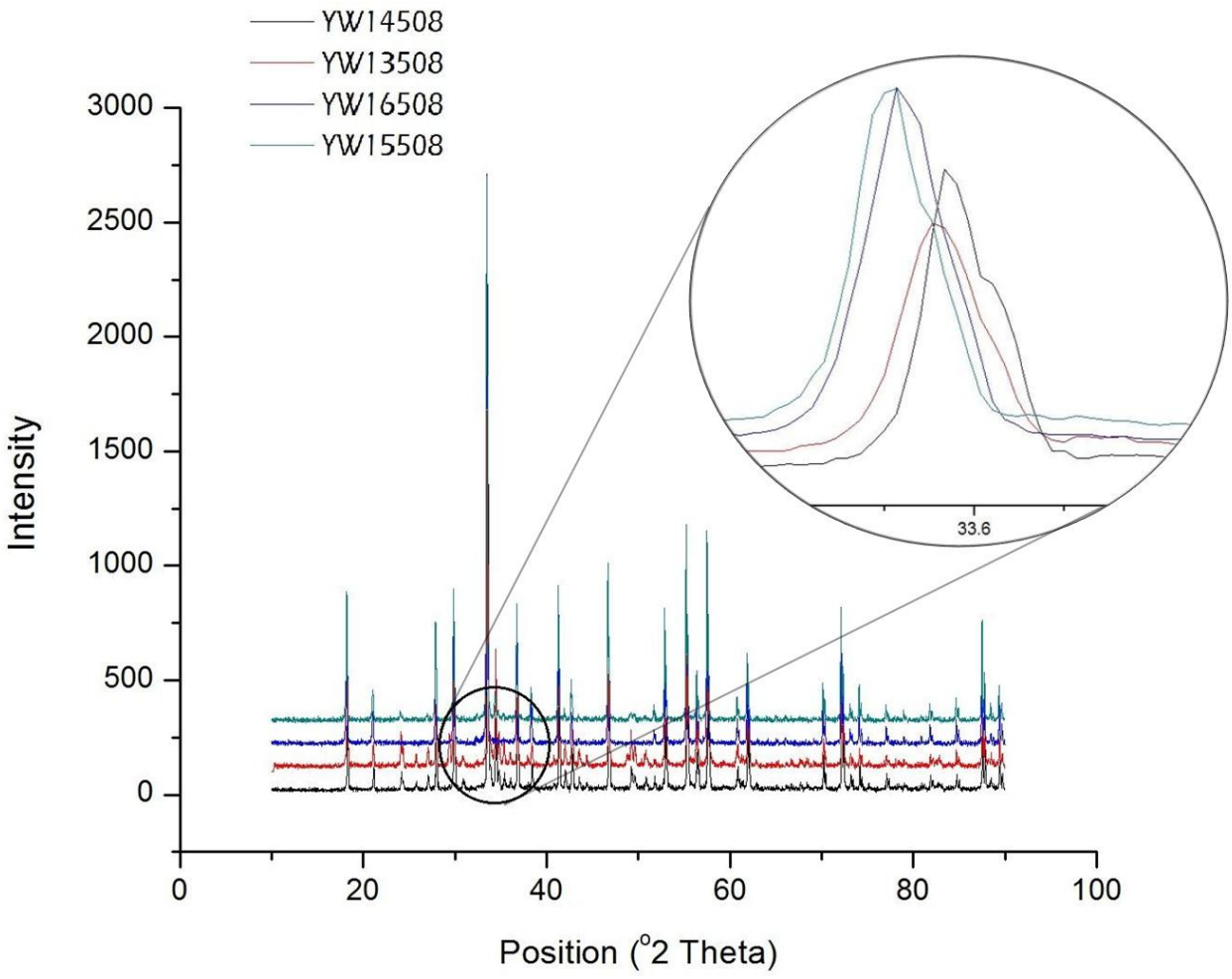

Fig. 4.1(e) *A comparative view of the x-ray diffraction patterns of various samples sintered at different temperatures such as 1350^{o}C, 1450^{o}C, 1550^{o}C and 1650^{o}C for a soaking time of 8 hours.*

In *figure 4.1(e)* the peak intensities reflect the total scattering from each plane in the phase's crystal structure, and are directly dependent on the distribution of particular atoms in the structure. Thus intensities are ultimately related to both the structure and composition of the

phase. The maximum peak intensity of YAG phase increases with the increase in sintering temperature. The shifting of peaks is caused due to development of residual stress in the crystal structure.

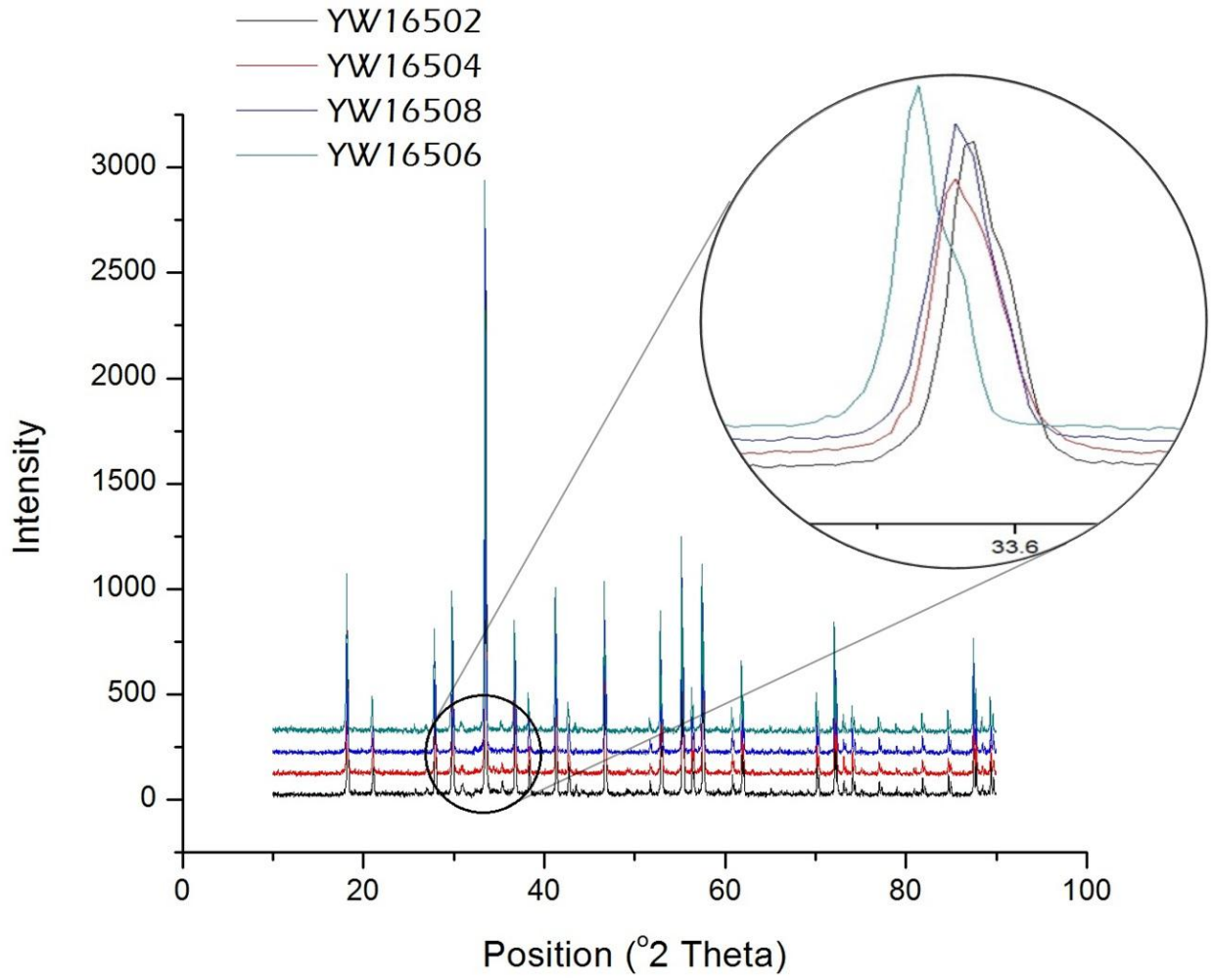

Fig. 4.1(f) *A comparative view of the x-ray diffraction patterns of various samples sintered at 1650°C for different soaking times such as 2hr, 4hr, 6hr and 8 hr.*

In *figure 4.1(f)* with the increase in soaking time there is an increase in grain size. This is evident from the fact that as the grain size increases the crystallite size increases and the peaks become narrower. The inter-atomic length increases with the growth of crystallites leading to the generation of strain and hence shifting of peaks is observed.

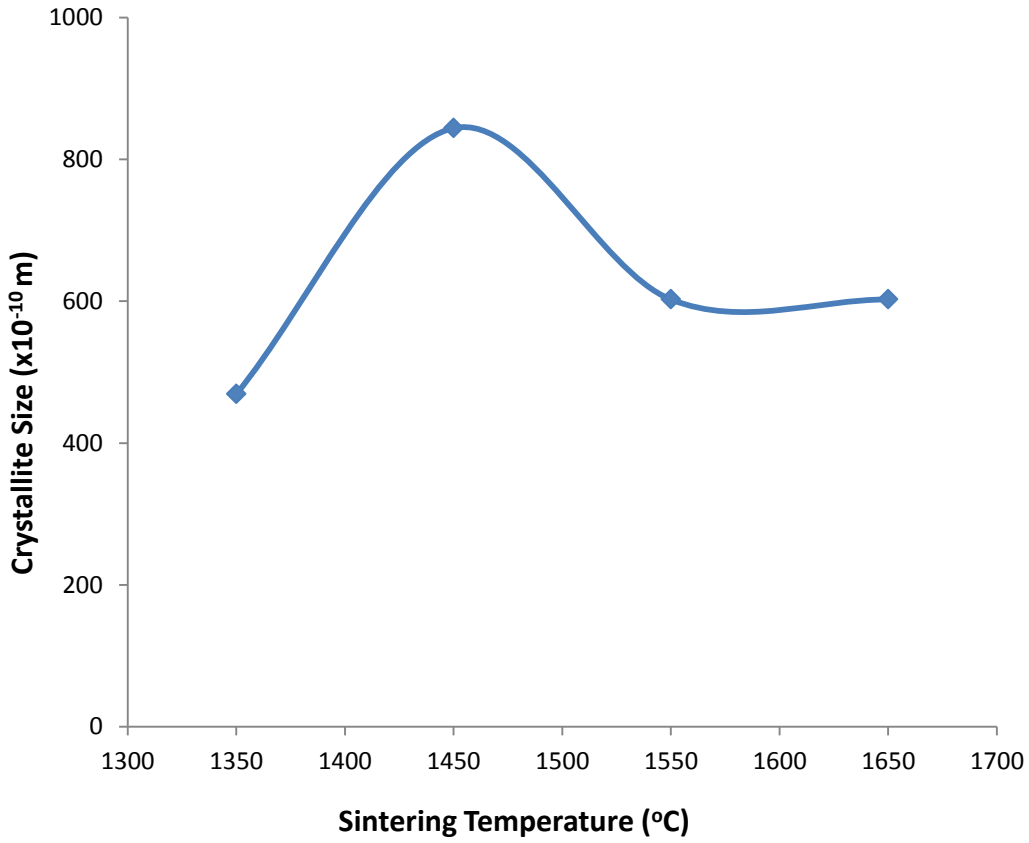

Fig 4.1(g) *Change in the crystallite size over sintering temperature.*

The graph in *figure 4.1(g)* has been derived from the XRD data of the preceding graphs using the Debye-Scherrer equation of determining the crystallite size given by

$$\text{Crystallite size,} \quad t = \frac{0.9\lambda}{B*\cos\theta_B}$$

The crystallite size follows a growth pattern from the temperature 1350^{o}C to 1450^{o}C, as expected, but falls abruptly at a higher temperature, 1550^{o}C and makes a steady rise to 1650^{o}C. This abnormality of decrease in crystallite size with increasing temperature can be addressed with the adoption of the dynamic recrystallization theory where grain size decreases with the increase in flow stress which can be given by the relation:

$$D=K\sigma^{-m}$$

K and m are material specific parameters.

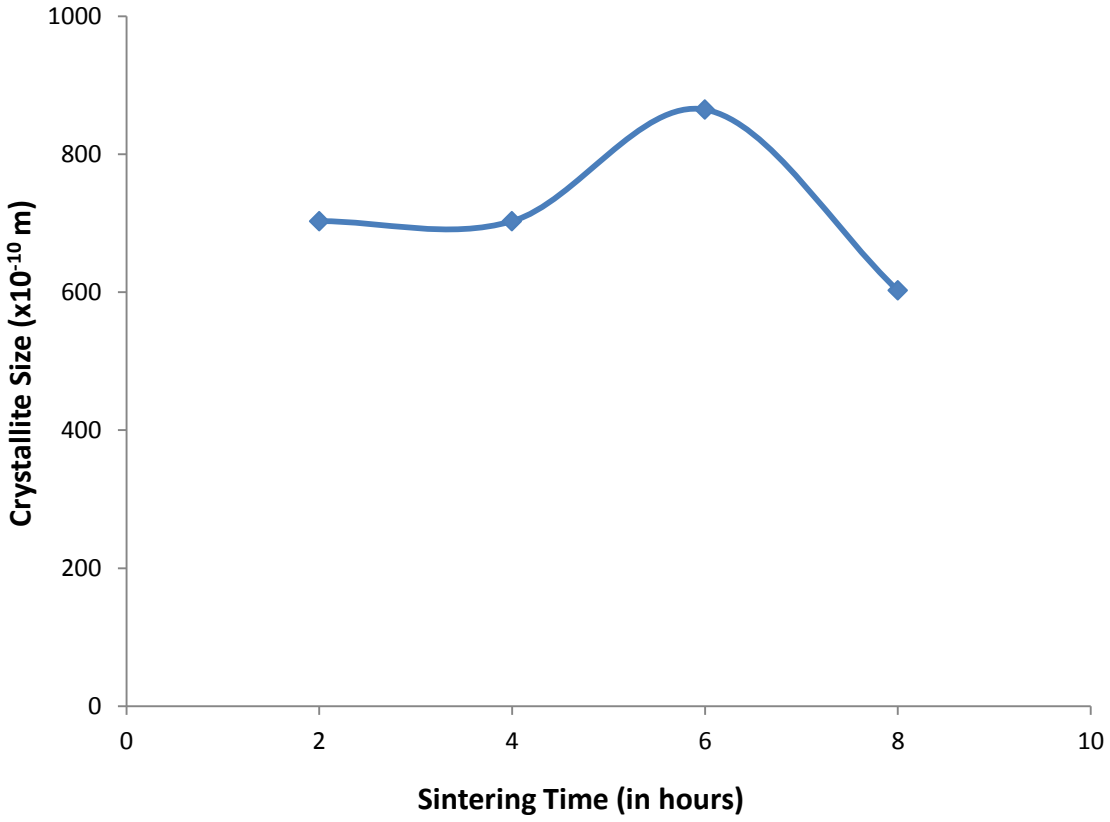

Fig 4.1(h) *Change in the crystallite size over soaking time at 1650^{o}C.*

In *figure 4.1(h)* the crystallite size increases with increase in soaking time but follows an abnormal decline at 1650^{o}C. This can be explained with the help of dynamic recrystallization theory explained above.

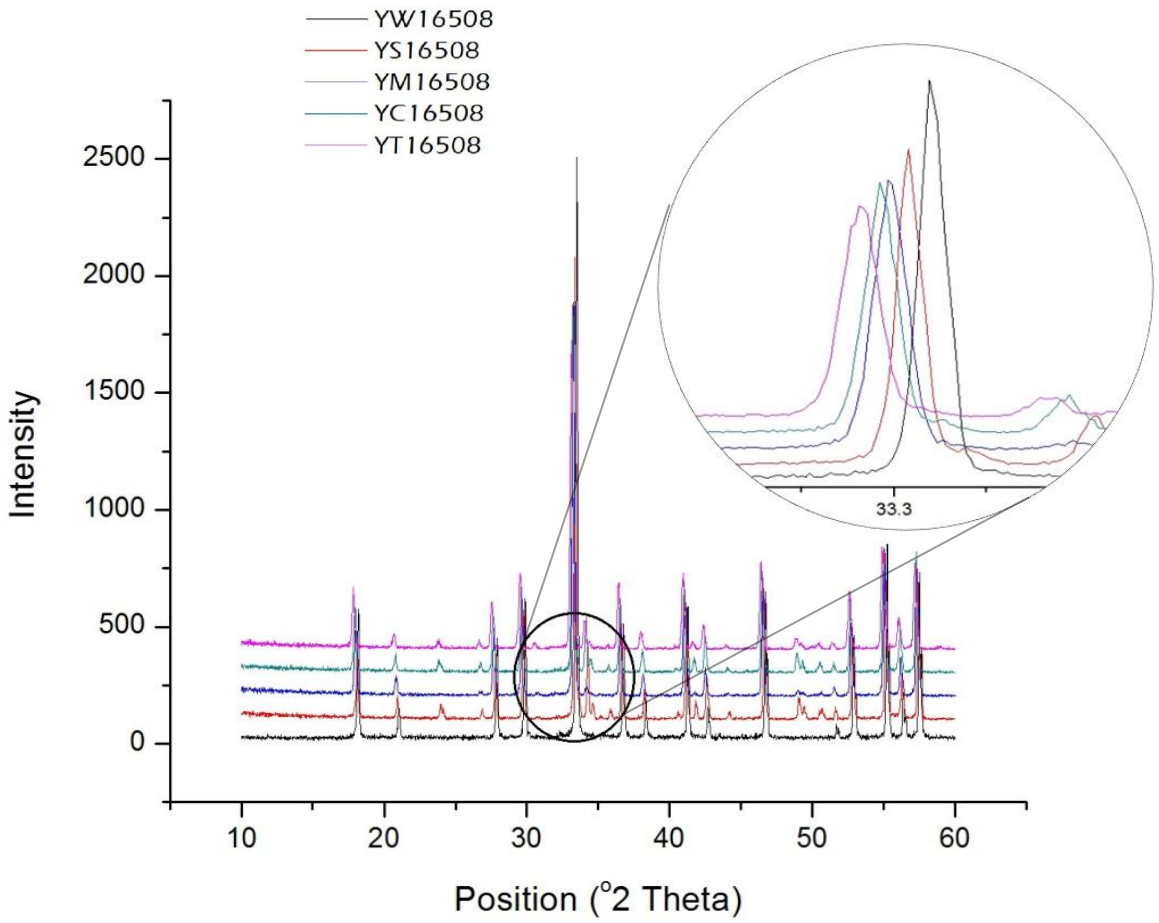

Fig. 4.1 (i) *A comparative view of the x-ray diffraction patterns of various YAG samples doped with 0.1 wt. % of different dopants and sintered at 1650^{o}C for 8 hours.*

The *figure 4.1 (i)* shows the phenomenon of peak narrowing as we scan through the range of dopants, giving us a hint of grain growth in the samples.

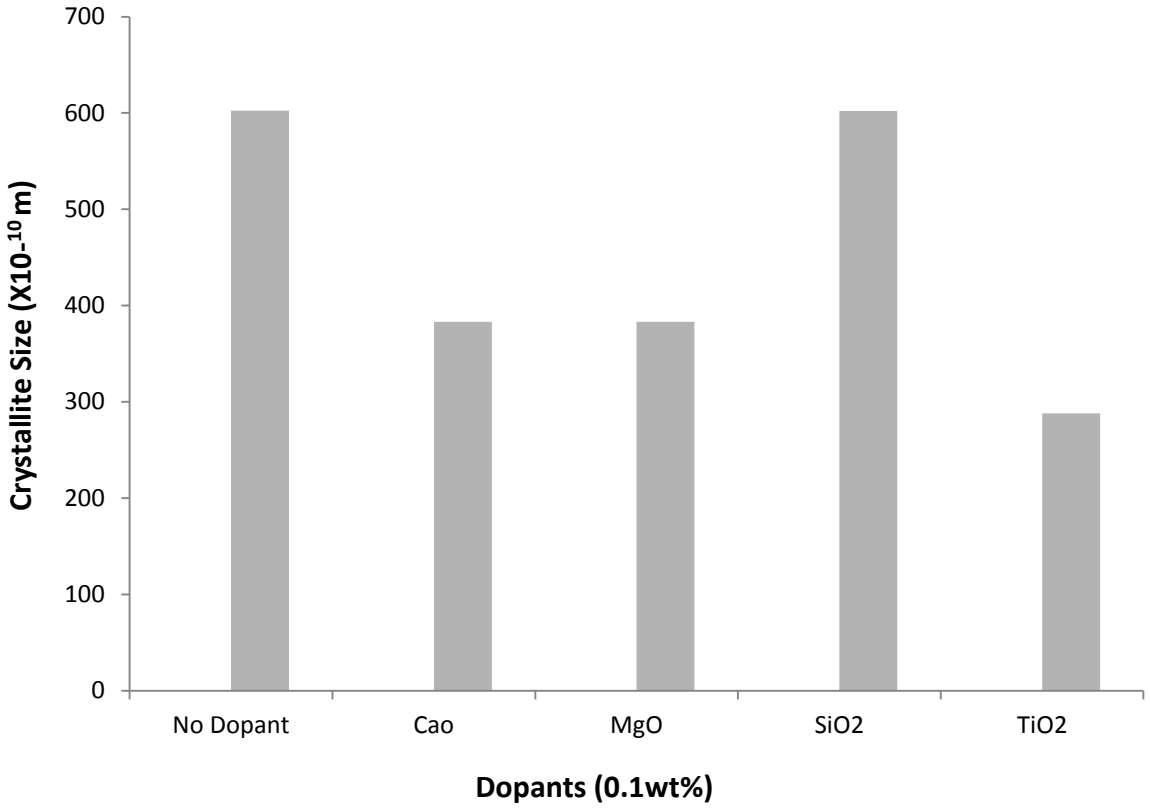

Fig 4.1(j) *Crystallite size of the samples sintered at 1650^{o}C with different dopants.*

In *figure 4.1(j)* 0.1 wt. % SiO_2 doped YAG shows a crystallite size of 60 nm which is quite high as compared to other doped samples. This gives an idea that considerable grain growth has occurred in case of SiO_2 doped sample. The association of the crystallite size of undoped YAG sample with the crystallite size of other doped samples could not be established.

4.2 SEM Micrography

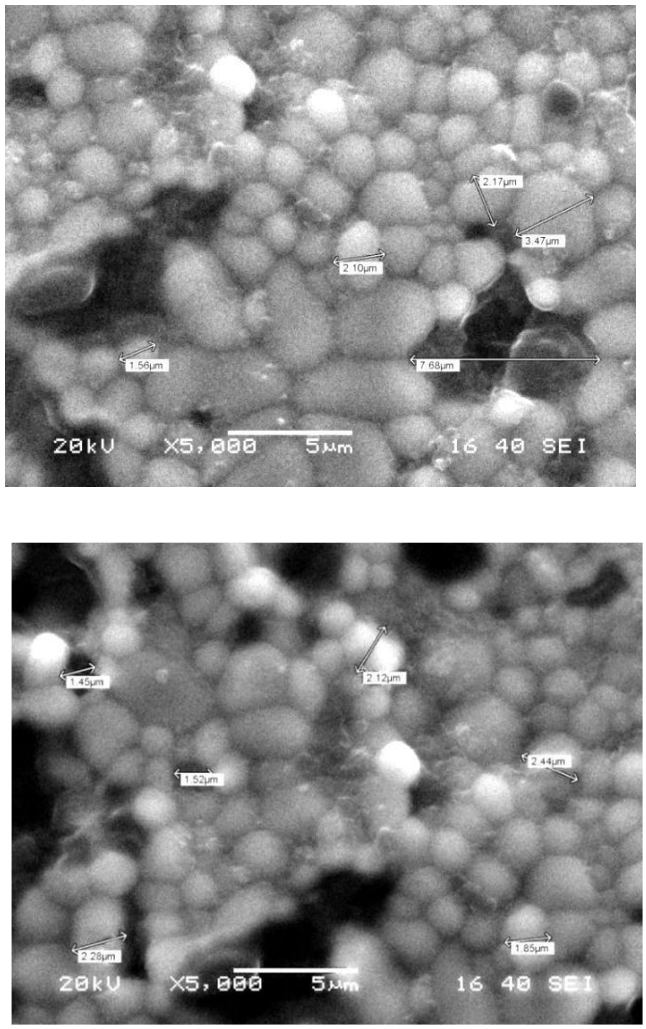

Fig.4.2 (a) *SEM micrographs of undoped YAG sample sintered at 1650^{o}C for 8 hours*

The average grain size of the sample in *figure 4.2(a)* is calculated from its SEM image by the linear intercept method for determining grain size and is found to be 1.67µm. Large sized pores are visible which is a result of incomplete densification. The grain size distribution spreads over a wide range.

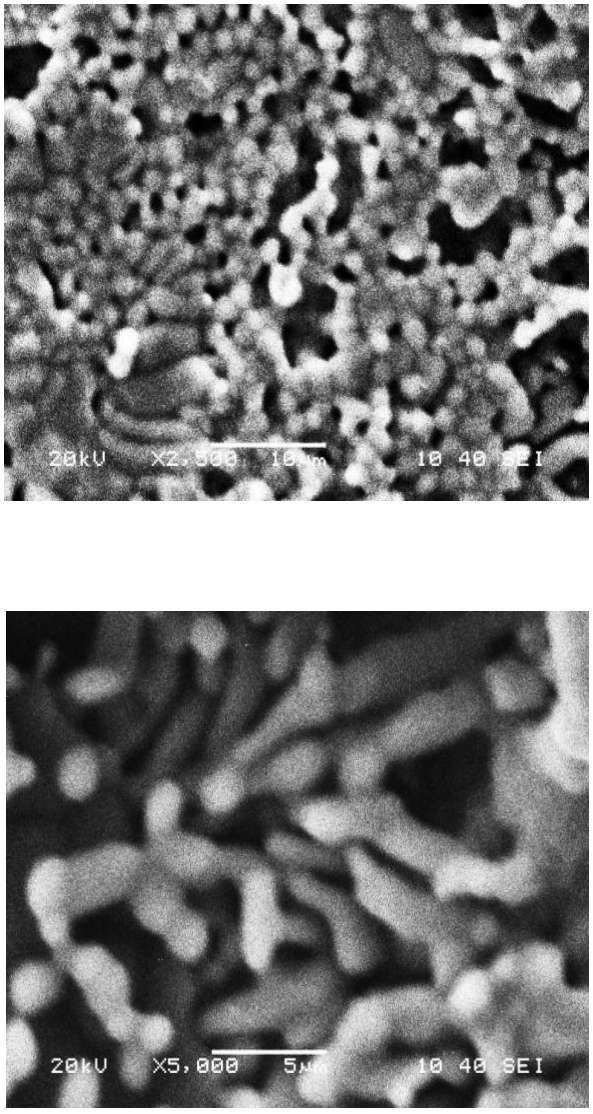

Fig.4.2 (b) *SEM micrographs of 0.1 wt. % SiO_2 doped YAG sample sintered at 1650^oC for 8 hours at different magnification levels.*

Figure 4.2 (b) evidently shows the occurrence of abnormal grain growth with the formation of grains that have a high aspect ratio. This results in a poor densification of the sample as evident from the bulk density and apparent porosity data that follows.

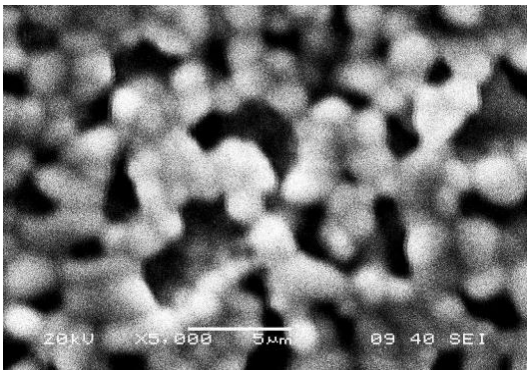

1650^{o}C

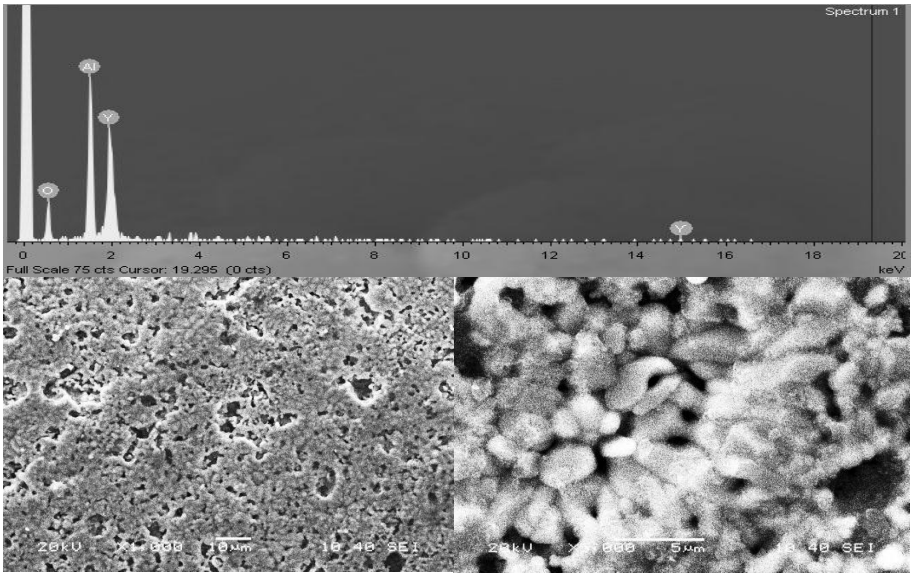

1550^{o}

Fig.4.2 (c) *SEM micrographs and EDAX spectra of 0.1 wt. % CaO doped YAG sample sintered at 1650^{o}C and 1550^{o}C for 8 hours at different magnification levels.*

Figure 4.2 (c) shows irregularly formed grains joining together in an incoherent manner giving rise to a body of low density and high porosity. The EDAX spectrum at 1550^{o}C shows peaks of elemental yttrium, aluminium and oxygen emitting varying intensities of x-rays specific to each element.

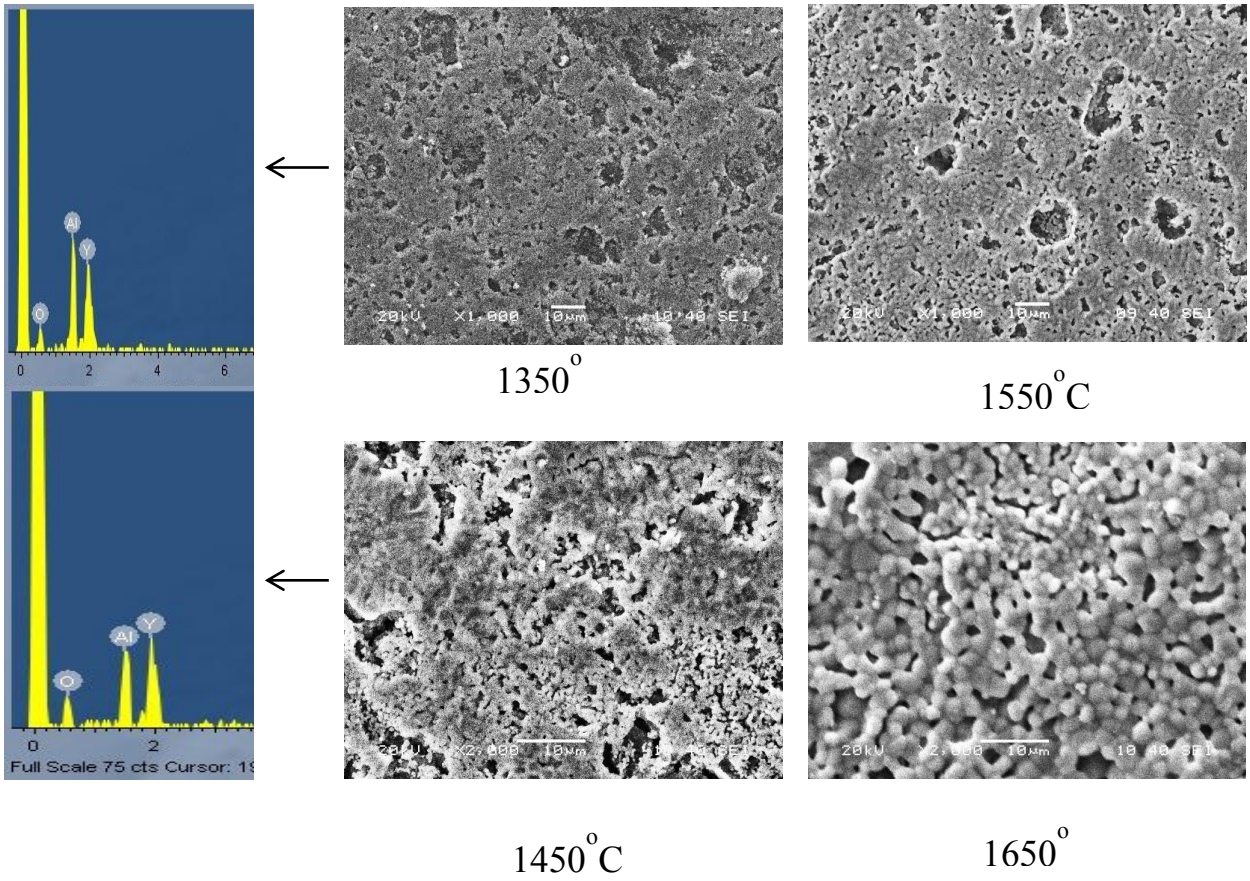

Fig.4.2 (d) *SEM micrographs of 0.1 wt. % MgO doped YAG sample sintered at 1350^{o}C, 1450^{o}C, 1550^{o}C and 1650^{o}C for 8 hours at different magnification levels with EDAX spectra for 1350^{o}C and 1450^{o}C sintered samples.*

In *figure 4.2 (d)* we observe a gradual fall in porosity with the increasing sintering temperature. At 1650^{o}C, more or less uniform grain morphology is obtained which leads to a higher bulk density of the sample. The EDAX spectrum shows the x-ray signatures of each of the elemental material from which the ceramic is made.

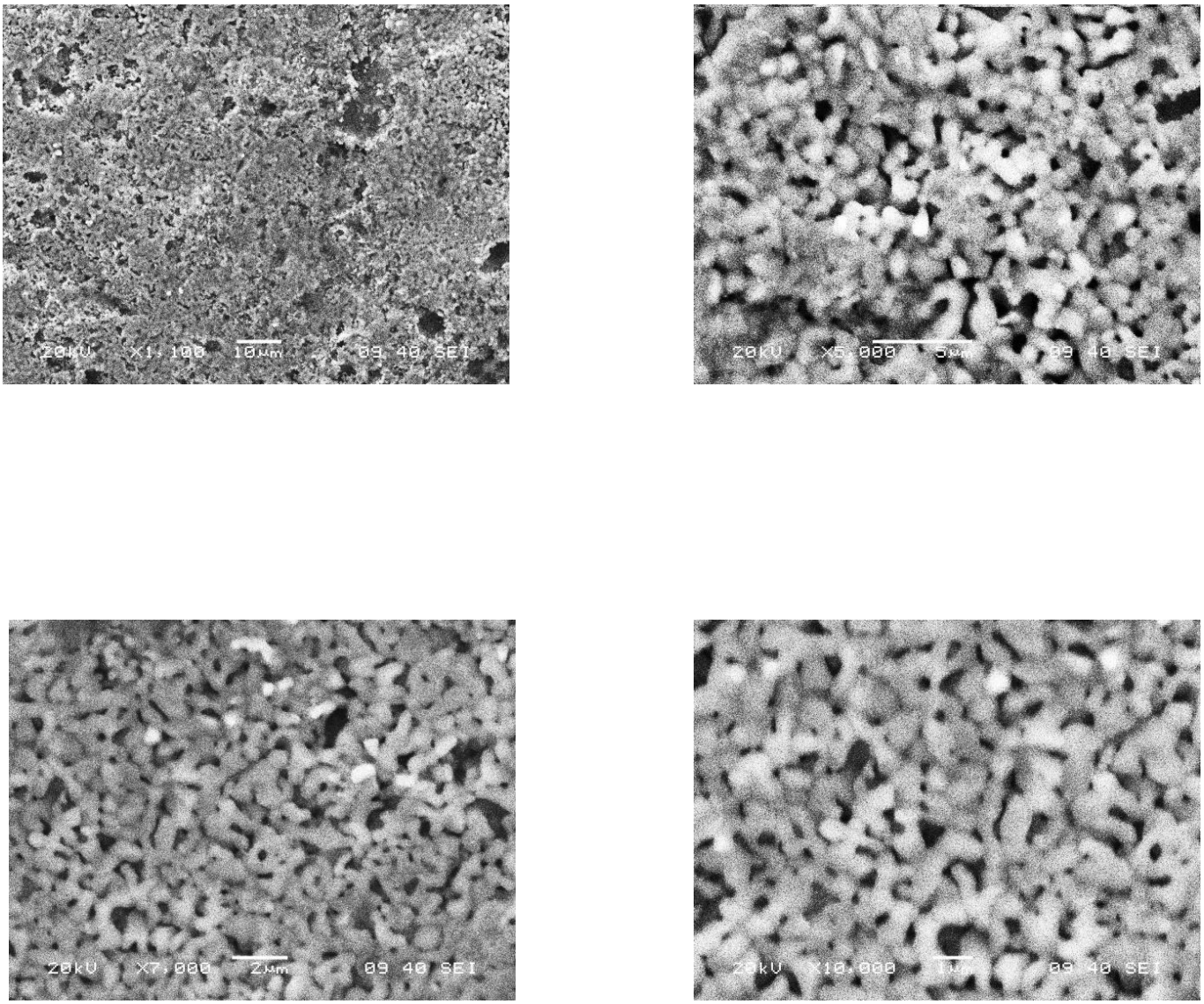

Fig.4.2 (e) *SEM micrographs of 0.1 wt. % TiO_2 doped YAG sample sintered at 1650^oC for 8 hours at different magnification levels.*

4.3 Bulk Density, Apparent Porosity and Shrinkage Measurements

Table 4.3(a) *Measurements of BD and AP for undoped samples sintered at different temperatures.*

Sample	Dry weight(in grams)	Suspended Weight(in grams)	Soaked weight(in grams)	Bulk Density(gm /cc)	Apparent Porosity (%)
YW13508	0.5426	0.416	0.6698	2.1379	50.1182
YW14508	0.5469	0.4233	0.6477	2.4372	44.9198
YW15508	0.546	0.4222	0.6402	2.5046	43.211
YW16508	0.507	0.3872	0.57	2.7735	34.4639

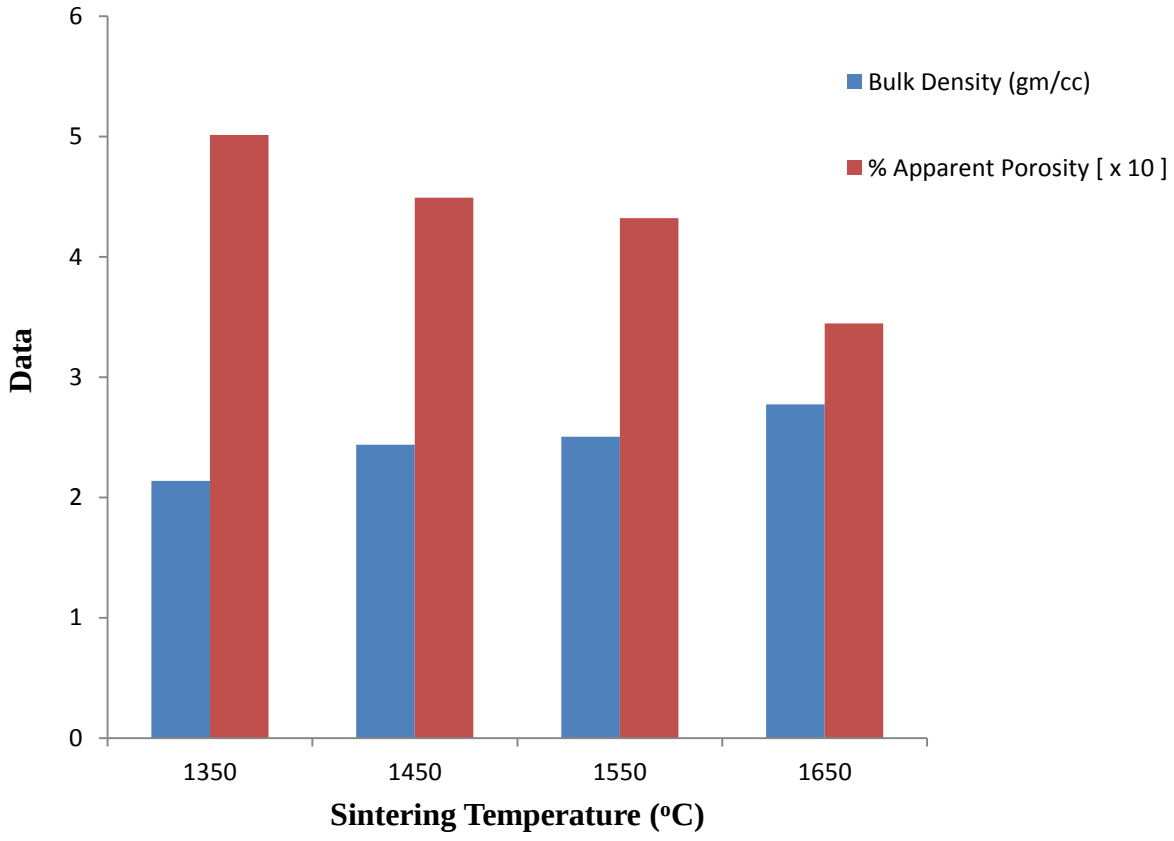

Fig.4.3 (a) *Change in bulk density and apparent porosity of undoped YAG samples with varying sintering temperatures.*

From *figure 4.3(a)* we observe that there is a steady increase in bulk density and decrease in apparent porosity as we move towards a higher sintering temperature hence giving the evidence of densification and removal of pores.

Table 4.3(b) *Measurements of BD and AP for undoped samples sintered at 1650^{o}C at different soaking times.*

Sample	Dry weight(in grams)	Suspended Weight(in grams)	Soaked weight(in grams)	Bulk Density(gm /cc)	Apparent Porosity (%)
YW16502	0.54	0.4073	0.6276	2.4512	39.764
YW16504	0.5339	0.41	0.6222	2.516	41.6117
YW16506	0.5428	0.415	0.6217	2.626	38.1713
YW16508	0.507	0.3872	0.57	2.7735	34.4639

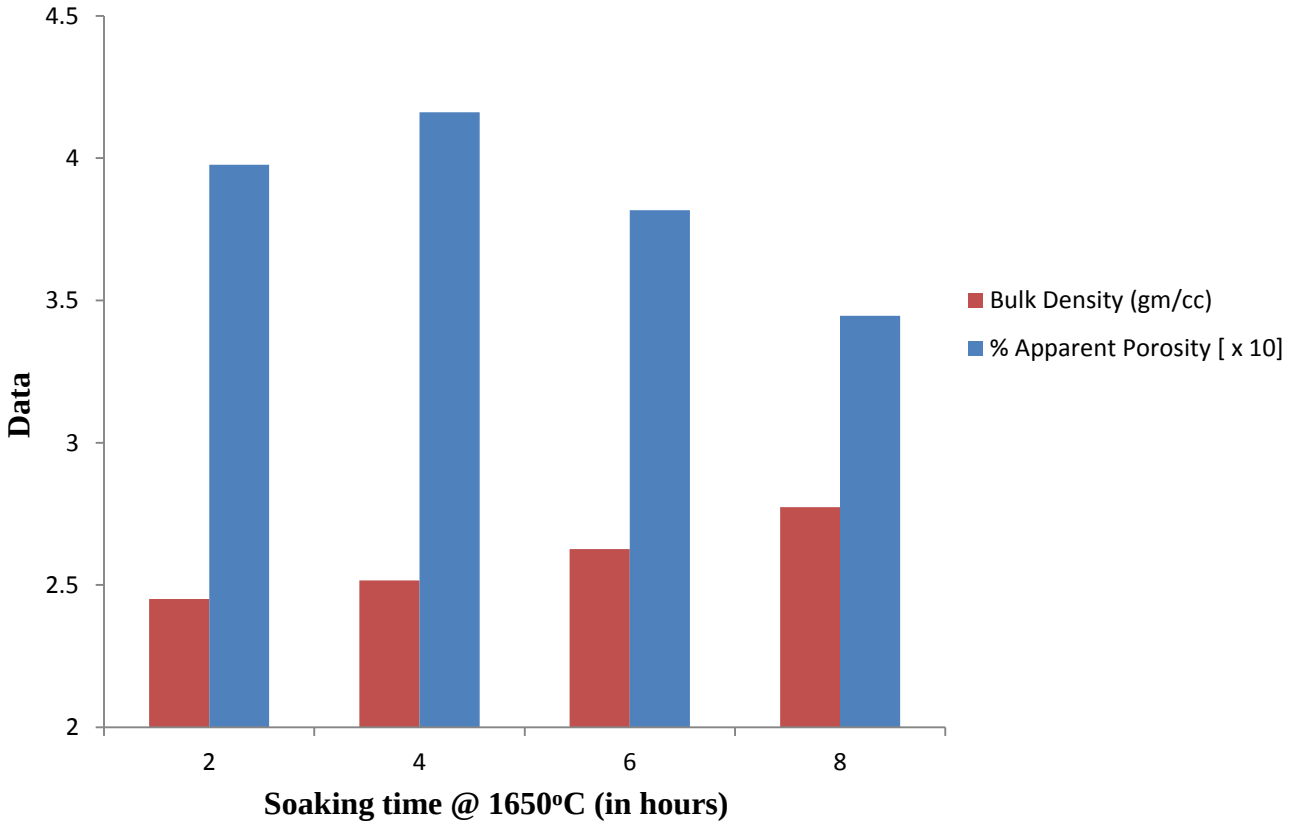

Fig.4.3 (b) *Change in bulk density and apparent porosity of undoped YAG samples (sintered at 1650^{o}C) with soaking time.*

From *figure 4.3(b)* we observe that there is a steady increase in bulk density and decrease in apparent porosity as we move towards a higher sintering temperature hence giving the evidence of densification and removal of pores.

Table 4.3(c) *Bulk Density data of YAG samples with different dopants.*

Sintering Temperature	Undoped YAG	0.1 wt.% CaO doped YAG	0.1 wt.% MgO doped YAG	0.1 wt.% SiO_2 doped YAG	0.1 wt.% TiO_2 doped YAG
1350 °C	0.5426	0.416	0.6698	2.1379	50.1182
1450 °C	0.5469	0.4233	0.6477	2.4372	44.9198
1550 °C	0.546	0.4222	0.6402	2.5046	43.211
1650 °C	0.507	0.3872	0.57	2.7735	34.4639

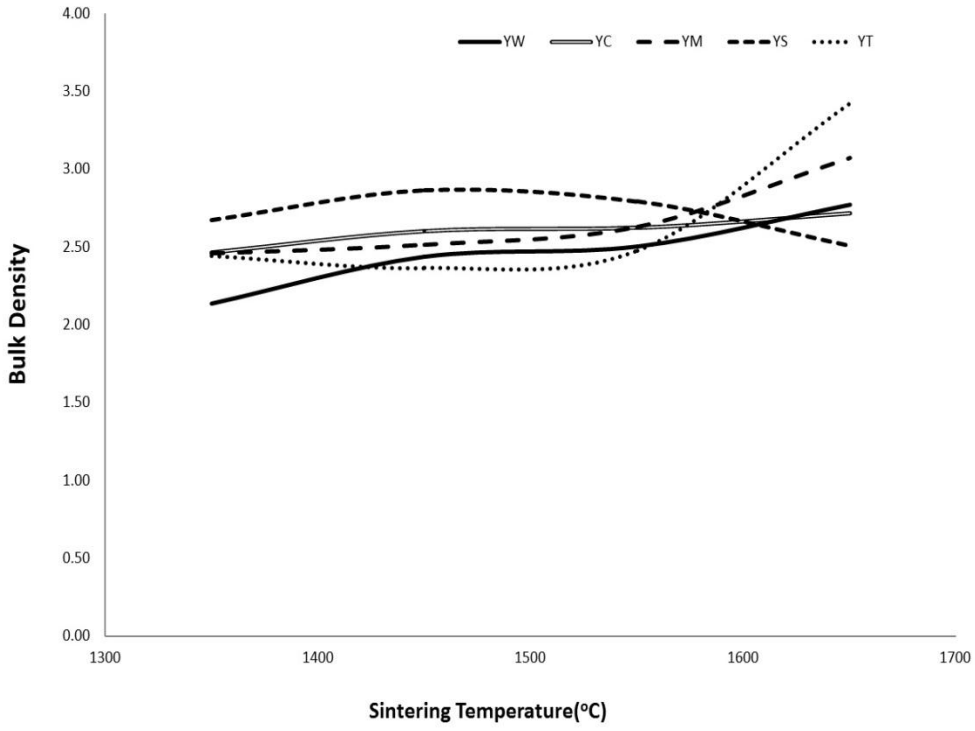

Fig.4.3 (c) *Change in bulk density of 0.1 wt. % of M_xO_y doped YAG with varying dopants and sintering temperatures.*

Table 4.3(d) *% Apparent Porosity data of YAG samples with different dopants.*

Sintering Temperature	Undoped YAG	0.1 wt.% CaO doped YAG	0.1 wt.% MgO doped YAG	0.1 wt.% SiO_2 doped YAG	0.1 wt.% TiO_2 doped YAG
1350 °C	50.1182	45.0688	48.1136	47.7520	49.4045
1450 °C	44.9198	46.5509	47.9471	48.2724	46.4513
1550 °C	43.211	45.3682	43.4025	42.2829	45.9714
1650 °C	34.4639	42.3265	32.9646	43.5839	40.9915

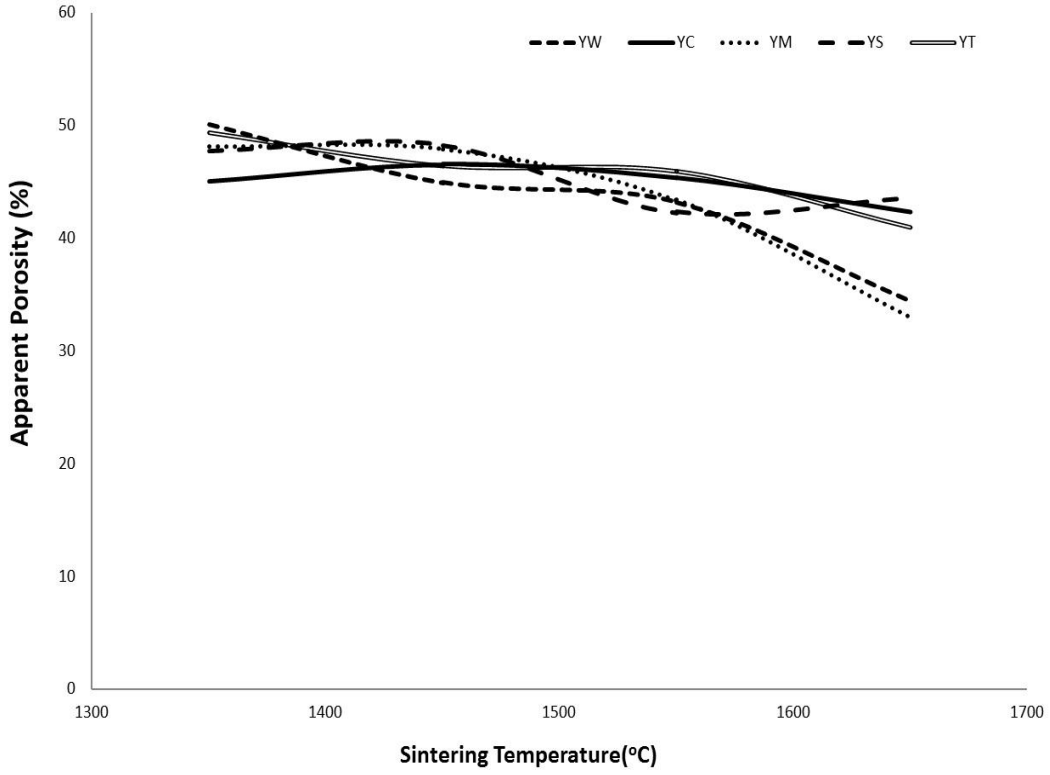

Fig.4.3 (d) *Change in apparent porosity of 0.1 wt. % of M_xO_y doped YAG with varying dopants and sintering temperatures*

.

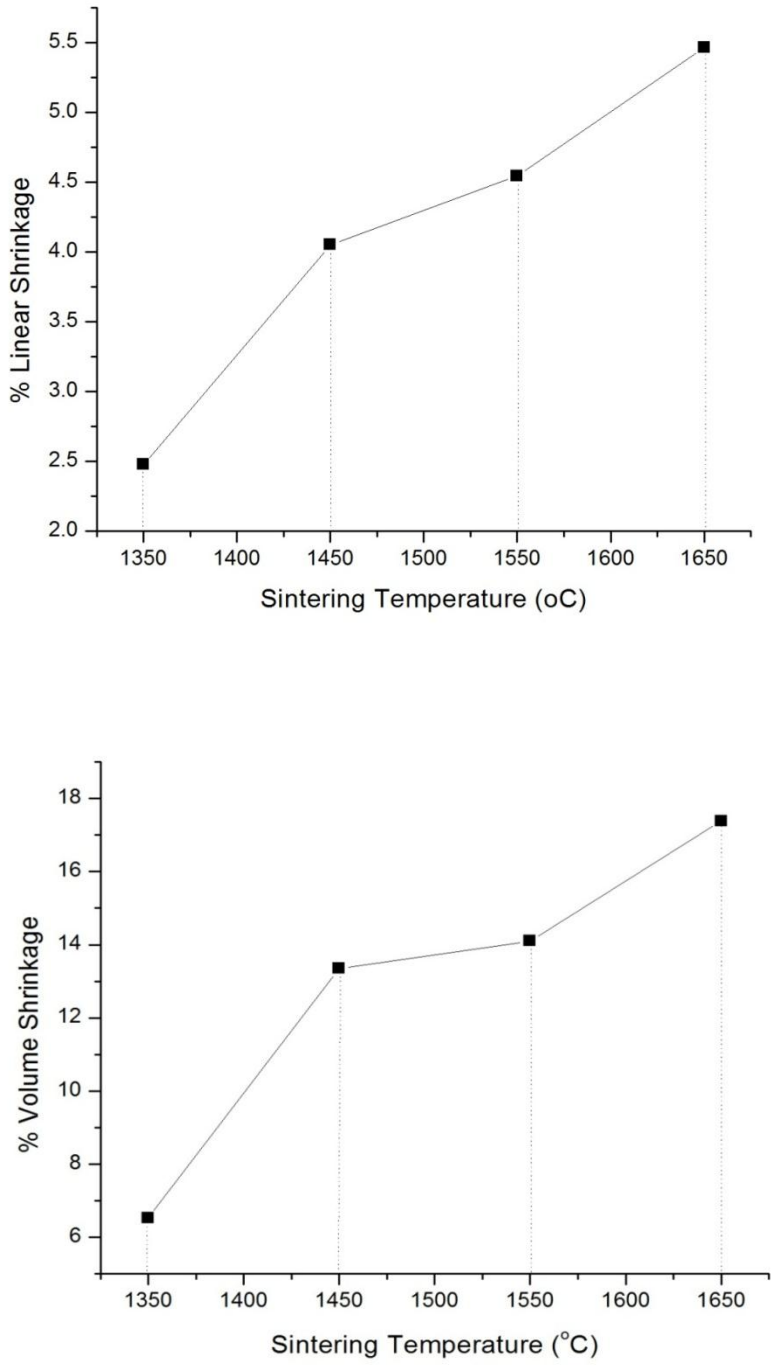

Fig.4.3 (e) *Dependence of linear and volume shrinkage of undoped YAG on sintering temperatures.*

4.4 Dilatometric Analysis

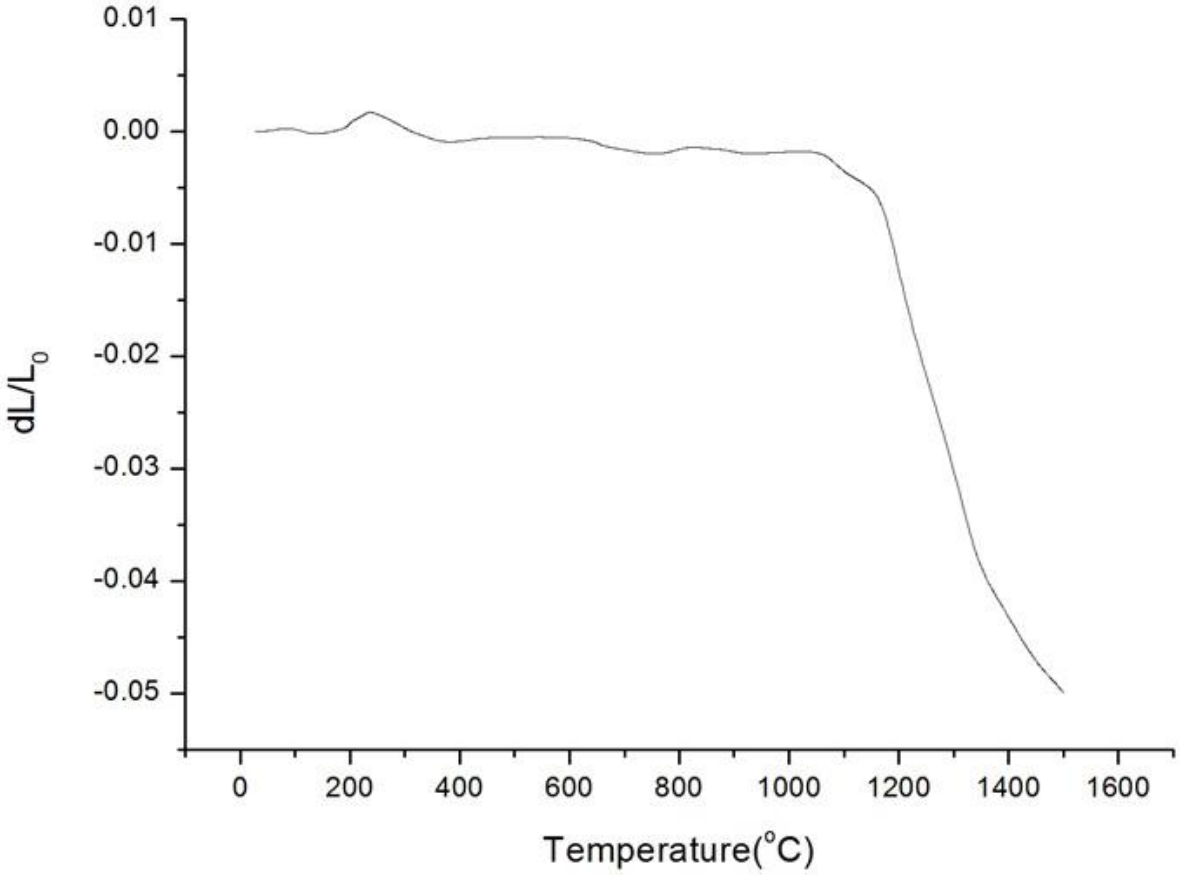

Fig. 4.4 *TMA thermogram of YAG precursors (Al_2O_3+Y_2O_3) heated till 1500°C.*

From *Figure 4.4* it is evident that the complete transformation of YAM to YAG phase hasn't been tracked as the firing was done only to a temperature of 1500oC whereas the YAP to YAG conversion takes place at a much higher temperature. Here the incomplete endotherm at a temperature of 1200°C signifies the transformation of low temperature YAM phase to YAP phase.

Conclusion

1) Polycrystalline YAG ceramics has been successfully prepared through solid-state sintering route with the addition of various oxide dopants.

2) The sample with 0.1 wt.% SiO_2 showed abnormal grain growth with increase in crystallite size with temperature. The bulk density follows a decline owing to incomplete densification.

3) The samples with 0.1 wt.% TiO_2 showed the highest density. Densification observed in the doped samples occurred primarily due to the phenomenon of liquid phase sintering.

4) The samples with 0.1 wt.% CaO and MgO showed irregular sized grain formation which packed in an incoherent manner leading to high amount of porosity and low bulk density. However MgO reaches considerable density at higher sintering temperature.

References

1. Website < http://lablemminglounge.blogspot.in>
2. *Yang, H., et al., Fabrication of Nd:YAG transparent ceramics with both TEOS and MgO additives.*
3. *Kochawattana, S., Lee, S.-H., Messing, G. L., Dumm, J. Q., Quarles, G. and Castillo, V., Solid-state reactive sintering of transparent polycrystalline Nd:YAG ceramics. J. Am. Ceram. Soc., 2006,* ***89****, 1945–1950.*
4. *Rahaman, M. N., Ceramic Processing and Sintering, 2nd Ed, CRC Press, 2003.*
5. *Yang, H., et al., Fabrication of Nd:YAG transparent ceramics with both TEOS and MgO additives.*
6. *Qing, L.C., Bo, Z.H., Fu, Z.M., Cai, H.J., He, M.S.: Fabrication of transparent YAG ceramics by traditional solid state reaction method, T. Nonferrous Metal Soc.,* ***17****, 148 – 153, (2007).*
7. *Kochawattana, S., Lee, S.-H., Messing, G. L., Dumm, J. Q., Quarles, G. and Castillo, V., Solid-state reactive sintering of transparent polycrystalline Nd:YAG ceramics. J. Am. Ceram. Soc., 2006,* ***89****, 1945–1950.*
8. *Esposito et al., Reactive sintering of YAG-based materials using micrometer-sized powders. Journal of the European Ceramic Society 28 (2008) 1065–1071.*
9. *Li, Y., Zhou, S., Lin, H., Hou, X., Li, W., Teng, T., Jia, T.: Fabrication of Nd:YAG transparent ceramics with TEOS, MgO and compound additives as sintering aids, J. Alloys Compd.,* ***502****, 225 – 230, (2010).*

10. *Wen, L., et al., Synthesis of Nanocrystalline Yttria Powder and Fabrication of Transparent YAG Ceramics, J. European Ceramic Soc., Vol. 24, p. 2681, (2004)*
11. *Yang, H., et al., The Effect of MgO and SiO_2 Co-doping on the Properties of Nd:YAG Transparent Ceramics, J. European Ceramic Soc.*
12. *Liu W et al., Synthesis of Nd:YAG powders leading to transparent ceramics: The effect of MgO dopant, J. European Ceramic Soc., Vol. 31, p. 653-657, (2011)*
13. *Coble, R. L., Transparent alumina and method of preparation.* ***US Patent*** *3026210, 20 March, 1962.*
14. *Tachiwaki, T., Yoshinaka, M. and Hirota, K., Novel synthesis of YAG leading to transparent ceramics. Solid. State. Communications, 2001, 119, 603–606.*
15. *De With, G. and Van Dijk, H. J. A., Translucent $Y_3Al_5O_{12}$ ceramics. Mater. Res. Bull., 1984, 29(12), 1669-1674.*